

A Novel Rabbit Dry Eye Model Induced by a Controlled Drying System

Xiao-Min Chen^{1,*}, Jian-Biao Kuang^{2,*}, Hui-Yin Yu¹, Zhen-Ning Wu¹, Shu-Yi Wang³, and Shi-You Zhou¹

¹ The State Key Laboratory of Ophthalmology, Zhongshan Ophthalmic Center of Sun Yat-sen University, Guangzhou, China

² Zhaoke (Guangzhou) Ophthalmic Pharmaceutical Co. Ltd, Guangzhou, China

³ School of Medicine, Sun Yat-Sen University, Guangzhou, China

Correspondence: Shi-You Zhou, The State Key Laboratory of Ophthalmology, Zhongshan Ophthalmic Center of Sun Yat-Sen University, Guangzhou, China. e-mail: zhoushiy@mail.sysu.edu.cn

Received: October 27, 2020

Accepted: March 13, 2021

Published: April 27, 2021

Keywords: dry eyes; rabbit; controlled drying system; dry eye model

Citation: Chen X-M, Kuang J-B, Yu H-Y, Wu Z-N, Wang S-Y, Zhou S-Y. A novel rabbit dry eye model induced by a controlled drying system. *Transl Vis Sci Technol.* 2021;10(4):32, <https://doi.org/10.1167/tvst.10.4.32>

Purpose: To establish an environment-induced dry eye model in rabbits using a controlled drying system (CDS).

Methods: Rabbits were randomly divided into two groups. The rabbits in the dry group were housed in the CDS, in which the relative humidity, airflow, and temperature were controlled at $22\% \pm 4\%$, 3 to 4 m/s, and 23°C to 25°C for 14 days. The rabbits in the control group were housed in a normal environment at the same time. A Schirmer test, fluorescein staining, and lissamine green staining were performed. On day 14, the eyeballs and lacrimal glands were processed for evaluating the corneal epithelial thickness, inflammatory cell infiltration index, goblet cell density, and expression of the MUC5AC protein and caspase-3 protein. The mRNA expression of the involved inflammatory genes was analyzed.

Results: The CDS was able to maintain a dry environment, in which the tear production decreased, and the ocular surface staining increased over time in the rabbits. In the dry group, the corneal epithelium became thinner, inflammatory cells were noted, goblet cells and MUC5AC proteins decreased, and the increased levels of caspase-3 proteins and inflammatory cytokines were observed in the ocular surface tissues and lacrimal glands.

Conclusions: This CDS could create a dry environment, in which the rabbits exhibited a pathological change in dry eye similar to that in humans.

Translational Relevance: This model would be helpful in offering a platform to identify and test candidate therapies for environment-induced dry eye and to explore its underlying mechanisms.

Introduction

Dry eye is a multifactorial disease of the ocular surface with discomfort symptoms and signs, such as ocular irritation and visual disturbance. A large number of human and animal studies have shown that dry eye can be induced by many internal or external factors, such as age, androgen deficiency, contact lenses, laser correction surgery, environmental pollution, and a low-humidity environment.^{1,2} When the tear film is unstable because of excessive evaporation, such as in low-humidity environment, the

lacrimal gland–ocular surface functional unit will be also damaged, and the individual will develop dry eye.³ Epidemiologic studies have found that 35% to 48% of people working in low-humidity conditions, such as offices, airplane cabins, and other air-conditioned rooms, suffer from dry eye.^{4–6} Therefore to further explore the pathogenesis of environment-induced dry eye, it is important to establish a model induced by low humidity.

In 2005, a murine dry eye model under low humidity ($18.5\% \pm 5.1\%$) and high airflow (15 L/min) induced by a controlled-environment chamber (CEC) was first established.⁷ This model showed signs similar

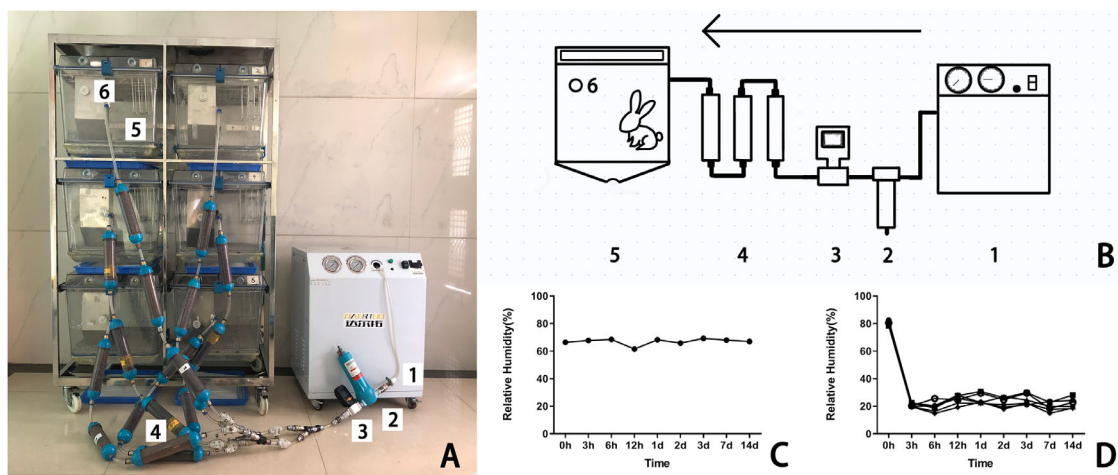


Figure 1. The real and illustrative structure of the CDS. **(A)** The CDS consisted of (1) an air pump, (2) a compressed air fine filter, (3) a flowmeter, (4) dry columns packed with desiccants, (5) a modified rabbit cage, and (6) a humidity recorder. **(B)** Schematic diagram of the CDS. The devices labeled 1 to 6 are referred to the same in the photograph A. **(C)** The RH of the air in the control group was steadily kept between 60% and 70%. **(D)** The RH of the air in the dry group was maintained at $22\% \pm 4\%$.

to patients with dry eye. Later, another study used the same principle to prepare a murine model of dry eye using an intelligently controlled environmental system (ICES),⁸ in which the relative humidity (RH), air flow (AF), and temperature (T) were maintained at $15.3\% \pm 3\%$, 2.1 ± 0.2 m/s, and 21°C to 23°C , respectively. However, it is difficult to observe clinical manifestations and detect the related biochemical indicators with the small size of murine eyeballs. In addition, there are some major differences between the eyes of mice and humans in terms of physiological and anatomic structure, as well as pharmacokinetic characteristics.⁹ Rabbits could offer significant advantages over other species because of the size of their eyeballs, their well-defined eyelid anatomy, the level of expression of drug-inactivating carboxylesterases, and their lacrimal gland histology, which are all closer to those of humans than mice.¹⁰ However, there have been no reports on environment-induced rabbit dry eye models until now.

In this study, we attempted to create a rabbit dry eye model in a consistently low-humidity environment using a controlled drying system (CDS), in which the RH, AF, and T could be remotely monitored and accurately adjusted. This model would be helpful in offering a good platform to identify and test candidate therapies for environmental dry eye and to further explore its underlying mechanisms.

Methods

Animals

All male white New Zealand rabbits weighing 2.0 to 2.5 kg were purchased from Guangzhou Baiyun

Longgui Xingke Animal Farm, Guangdong, China. The rabbits were kept in quarantine and acclimatized for 1 week before the study at Sun Yat-sen University (Guangzhou, China). The rabbits were numbered and housed in a normal living habitat (RH, 60%–70%; T, 23°C – 25°C ; AF, 0.2 m/s) after the dissection of nictitating membrane for at least 1 week before the experiment. Then they were randomly assigned into either the dry group or the control group equally according to the random sequence ($n = 12$ each). All procedures were performed following the ARVO Statement for the Use of Animals in Ophthalmic and Vision Research. The protocol was approved by the Sun Yat-sen University Institutional Animal Care and Use Committee (approval number: SYSU-IACUC-2019-000028).

The CDS

The structure of the CDS used in this study is shown as Figure 1. It was mainly comprised of an air pump (MDET550; Wenling Shenba Co. Ltd., Zhejiang, China), a compressed air fine filter (015P; Lin-an Xinlei Mechanical and Electrical Equipment Co. Ltd., Hangzhou, China), a flow meter (MF5712, Siargo MEMS Co. Ltd., Lexington, MA), dry columns (Yuxin Environmental Protection and Technology Co. Ltd., Guangdong, China), and rabbit cages ($50 \times 60 \times 56$ cm) that were based on the size of rabbit and the requirement of animal ethics. An iron mesh isolation layer was added to the upper layer of each rabbit cage where desiccants (Guangdong Hongxiang Co. Ltd., Guangdong, China) were placed. The detachable bottom of each rabbit cage was grooved for the removal of rabbit excrement, featuring a hole for air and rabbit urine discharge. Each cage was monitored by a

humidity recorder (Xiaomi Technology Co. Ltd., Beijing, China). AF was provided via a low noise (45 dB) air pump with a compressed air fine filter, a flow meter, and a valve and detected by an anemometer with an accuracy of $\pm 1\%$ (HT-9829; Xintai Instruments and Apparatuses Co. Ltd., Guangdong, China).

Animals in the dry group were housed in the CDS, where the relative RH, AF, and T were controlled at $22\% \pm 4\%$, 3 to 4 m/s, and 23°C to 25°C , respectively, to achieve the best modeling conditions. The control group was still kept in a normal environment. The rabbits in both groups were evaluated using the following indicators on days 0, 3, 7, and 14.

Measurement of Aqueous Tear Production

Aqueous tear production was measured by Schirmer paper strips (Liaoning Meizilin Pharmaceutical Co. Ltd.; Liaoning, China). After topical anesthesia with 1% proparacaine hydrochloride eyedrops (Nanjing Ruinian Baisite Pharmaceutical Co. Ltd.; Jiangsu, China), a Schirmer paper strip was inserted into the peripheral conjunctival sac of rabbit eyes for 5 minutes. The length of the paper strip with the color change was measured.

Corneal Fluorescein Staining and Conjunctival Lissamine Green Staining

Corneal fluorescein staining and conjunctival lissamine green staining were performed with the staining paper strips (Liaoning Meizilin Pharmaceutical Co. Ltd.) and photographed under a slit-lamp microscope with a cobalt blue filter for the fluorescein staining and a yellow filter for the lissamine staining. The corneal fluorescein staining was graded by a standardized grading system (National Eye Institute),¹¹ whereas the superior bulbar conjunctival staining with lissamine green was graded from 0 to 5 according to the Oxford scheme.¹²

Histologic Analysis of Cornea, Conjunctiva, and Lacrimal Gland

Four rabbits (eight eyes) per group were made into paraffin cut sections. The sections were stained with a hematoxylin and eosin (HE) reagent or periodic acid-Schiff (PAS) reagent.¹³ The inflammatory cells and goblet cells were observed and calculated at nine random visual fields under $400\times$ magnification by an image analyzing system (AxioPlan 2 imaging, Zeiss, Oberkochen, Germany) and then analyzed by Image J 1.8.0 (National Institutes of Health, Bethesda, MD).

The thickness of the corneal epithelium was calculated as the average of three measurements at the medial point. The degree of inflammatory infiltration refers to the percentage of inflammatory cells.

Immunofluorescence Staining for MUC5AC Protein

Immunofluorescence staining of the MUC5AC protein on the superior bulbar conjunctiva of three rabbits (six eyes) per group was performed.¹⁴ The sections were deparaffinized, dehydrated, and washed, which was followed by antigen retrieval with a citrate antigen retrieval solution (P0081, Beyotime Biotechnology Co. Ltd., Shanghai, China). The sections were blocked with 10% goat serum at room temperature for 2 hours and incubated at 4°C for 12 hours with a 1:100 mouse anti-rabbit MUC5AC antibody (ab212636; Abcam, Cambridge, UK). After three washes in phosphate buffered saline (PBS), an anti-mouse IgG (H+L) F(ab')₂ fragment antibody (4408S; Cell Signaling Technology, Inc., Danvers, MA) was added to the specimens and incubated at room temperature for 2 hours. This was followed by three washes in PBS; then DAPI (F6057; Sigma-Aldrich, St. Louis, MO) staining was performed. Meanwhile, to demonstrate the specificity of anti-MUC5AC antibody, the antibody was substituted by isotype control antibody (ab170190; Abcam) to finish the control experiment. The specimens were examined at $200\times$ magnification by an epifluorescence microscope (AxioPlan 2 imaging; Zeiss).

Evaluation of Apoptosis in Cornea, Conjunctiva, and Lacrimal Gland

Immunohistochemistry was performed to detect the caspase-3 protein to evaluate the cellular apoptosis in the cornea, conjunctiva, and lacrimal gland of three rabbits (six eyes) per group.¹¹ The sections were deparaffinized, rehydrated, and processed for antigen retrieval in the same way as described earlier. Then they were placed in 3% H₂O₂ for 10 minutes and washed with distilled water. After that, they were placed in diluted goat serum for 1 hour and then washed three times in PBS. The tissue samples were incubated with 1:100 polyclonal mouse anti-caspase-3 antibody (ab208161; Abcam) at 4°C overnight and then incubated with a goat anti-mouse secondary antibody (ab97040; Abcam) for 2 hours at room temperature. Diaminobenzidine (DAB) staining was performed after three washes in PBS. Meanwhile, the antibody was replaced by isotype control antibody

Table. Primer Sequences for Real-Time qPCR in the Rabbit

Gene	Primer Sequence	Product (bp)
GAPDH	GAACGGGAAACTCACTGG CTTCACCTTCTTGATGT	115
IL-1 β	CTCCATGAGCTTTGTACAAGG TGCTGATGTACCAGTTGGGG	245
TNF- α	ATGGTCACCTCAGATCAGCTTCT AAGAGAACCTGGGAGTAGATGAGG	200
MMP9	CCTGCGAGTTTCCGTTCA AGCCGTAGAGCTTGTCTTG	123

(ab170190; Abcam) to complete the control experiment to demonstrate the specificity of anti-caspase-3 antibody. Apoptotic cells with positive staining were detected under 400 \times magnification by an image analyzing system (Axioplan 2 imaging; Zeiss). The relative integrated optical density (IOD) of the protein expression was analyzed using Image-Pro Plus 6.0 (Media Cybernetics, Rockville, MD).

Real-Time Quantitative Polymerase Chain Reaction Analysis

The mRNA expression levels of interleukin (IL)-1 β , tumor necrosis factor (TNF)- α , and matrix metalloproteinase 9 (MMP-9) in the cornea, conjunctiva, and lacrimal gland were detected via real-time quantitative polymerase chain reaction (qPCR). On the 14th day, 5 rabbits (10 eyes) per group were euthanized. The total RNA of each sample was immediately isolated using a TRIZOL reagent (15596-026; Invitrogen, Carlsbad, CA) according to the manufacturer's protocol, as described previously. After the quantification of the total RNA concentration, 2- μ g RNA was used to synthesize cDNA using the PrimeScript RTreagent kit (DRR037A; Takara, Mountain View, CA). The results were analyzed using a Roche Light-Cycler 480 (Roche Diagnostics Corporation, Indianapolis, IN). Each sample was run in triplicate. PCR was conducted in a 20- μ L reaction system, which contained 10- μ L SYBR Premix Ex Taq (DRR420A; Takara), a 0.4- μ L PCR Forward primer (D3801; Takara), a 0.4- μ L PCR Reverse primer (D3802; Takara), 2- μ L cDNA as the original template, and 7.2- μ L ddH₂O. Thermal cycling consisted of denaturation for 30 seconds at 95°C followed by 40 cycles of 10 seconds at 95°C, 1 minute at 60°C, and 30 seconds at 50°C for cooling. The PCR amplification efficiency of the primer sets was determined to be 100% before qPCR. The expression of GAPDH gene was used as an internal reference. The relative expression level of IL-1 β , TNF- α , and MMP-

9 mRNA was computed using the $2^{-\Delta\Delta C_t}$ method. The primer sequences used are listed in the [Table](#).

Statistical Analysis

Statistical analysis was performed using SPSS 20.0 (SPSS Inc, Chicago, IL) and illustrated using GraphPad Prism 6.0 (GraphPad Software, San Diego, CA). The quantitative data with normal distributions were expressed as mean \pm standard deviation (SD). When the differences between the two groups at different time points had normally distributed data and homogeneous variance, a repeated-measurement analysis of variance (ANOVA) test was used, whereas a corrected repeated-measurement ANOVA test was used when the variance was heterogeneous. When the differences between the two groups during the experiment days presented normally distributed data and homogeneous variance, the independent sample Student's *t*-test was used. A *P* value of less than 0.05 was considered statistically significant.

Results

Environmental Conditions Under the CDS

The overall structure of the CDS is shown in [Figures 1A, 1B](#). The RH and AF of the normal environment were kept at 60% to 70% ([Fig. 1C](#)) and 0.2 *m/s*, whereas those of the CDS were controlled at 22% \pm 4% ([Fig. 1D](#)) and 3 to 4 *m/s* during the experimental period. When the cage was opened for the provision of food or cleaning for approximately 10 minutes a day, the humidity level inside the cage would increase rapidly and then recover to the original settings within 2 to 3 hours. The temperature of the CDS was set to room temperature (23°C–25°C).

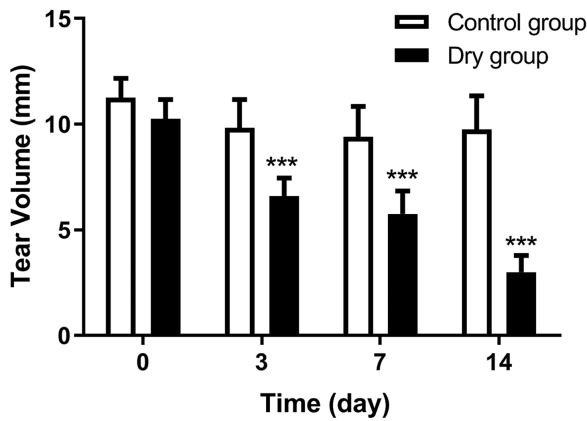


Figure 2. The results of the Schirmer's test at different checkpoints. The tear volume of the dry group decreased over time from day 3 and was statistically fewer than that of the control group (all *** $P < 0.001$, $n = 12$ [24 eyes] per group). Data are shown as mean \pm SD (error bars).

Animal Behavior Under the CDS

Neither the rabbits in the control group or the dry group showed any abnormal activities or changes, such as weight loss, moult, or frequent eye rubbing, during the experimental period. The amount of food and water consumed in the two groups was similar (data not shown).

Aqueous Tear Production

A Schirmer's test was used to quantify the tear production. Before the experiment, the tear volume of the control group and dry group were 11.3 ± 1.0 mm and 10.3 ± 0.9 mm, respectively, indicating no statistical differences between the two groups at baseline. The Schirmer test measurements in the control and dry groups were 9.8 ± 1.4 mm and 6.6 ± 0.9 mm on day 3, 9.4 ± 1.5 mm and 5.8 ± 1.1 mm on day 7, and 9.8 ± 1.6 mm and 3.0 ± 0.8 mm on day 14, respectively. There were statistical differences between the two groups at each time point (ANOVA, $F = 110.962$, $P < 0.0001$, $n = 12$ [24 eyes] per group). The tear production of the dry group gradually decreased with time on days 3, 7, and 14 when compared with baseline (Bonferroni method, all $P < 0.001$, $n = 12$ [24 eyes] per group, Fig. 2).

Corneal Fluorescein Staining and Conjunctival Lissamine Green Staining

The degree of corneal and conjunctival epithelial damage can be evaluated via corneal fluorescein staining and conjunctival lissamine green staining, respectively, according to the National Eye Institute grading systems and the Oxford scheme.^{14,15}

There were no statistical differences between the control and dry groups in terms of the fluorescein staining scores (1.2 ± 0.9 vs. 1.2 ± 0.9 , respectively) at baseline (Fig. 3A). On days 3, 7, and 14 of the experiment, the corneal fluorescein staining scores were 1.3 ± 0.8 versus 4.7 ± 1.5 , 1.3 ± 0.9 versus 5.5 ± 1.6 , and 1.0 ± 0.7 versus 8.5 ± 2.1 in the control group and dry group, respectively (Figs. 3B–D). There were statistical differences between the two groups at each time point (repeated measurement ANOVA, $F = 60.558$, $P < 0.0001$, $n = 12$ [24 eyes] per group). The corneal fluorescein staining scores in the dry group gradually increased with time (Bonferroni method, all $P < 0.001$, $n = 12$ [24 eyes] per group, Fig. 3I).

The conjunctival lissamine green staining scores were 0.2 ± 0.4 versus 0.1 ± 0.3 , 0.1 ± 0.3 versus 0.8 ± 0.8 , 0.2 ± 0.4 versus 1.0 ± 1.0 , and 0.2 ± 0.4 versus 2.0 ± 1.1 in the control group and dry group, respectively, on days 0, 3, 7, and 14 (Figs. 3E–H). Additionally, there were statistical differences between the two groups at each time point (repeated measurement ANOVA, $F = 29.137$, $P < 0.0001$, $n = 12$ [24 eyes] per group). The conjunctival lissamine green staining scores in the dry group gradually increased on days 3, 7, and 14 (Bonferroni method, $P < 0.05$, $P < 0.01$, $P < 0.001$, respectively, $n = 12$ [24 eyes] per group, Fig. 3J).

Histological Change in Cornea, Conjunctiva, and Lacrimal Gland

On day 14, there were 5 to 6 layers of corneal epithelial cells in the control group, whereas there were 3 to 4 layers in the dry group (Figs. 4A, 4B). The thickness of the corneal epithelium in the dry group was significantly decreased compared with that in the control group (47.8 ± 7.6 μm vs. 58.0 ± 7.2 μm , respectively, $t = 2.469$, $P < 0.05$, $n = 4$ [8 eyes] per group, Fig. 4C).

Histopathological analysis of the conjunctiva and lacrimal gland revealed that there was a more significant increase in the number of infiltrated inflammatory cells in the dry group than in the control group. Moreover, the index of inflammation in the dry group was significantly higher than in the control group (conjunctiva: $26.16\% \pm 1.1\%$ vs. $21.70\% \pm 2.7\%$, respectively; $t = -2.646$, $P < 0.05$, $n = 4$ [8 eyes] per group, Fig. 4F; lacrimal gland: $15.55\% \pm 4.6\%$ vs. $10.11\% \pm 2.4\%$, respectively; $t = -2.338$, $P < 0.05$, $n = 4$ [8 eyes] per group, Fig. 4I).

Density of the Goblet Cells and Expression of the MUC5AC Protein

The conjunctival goblet cells presented with positive PAS staining, which is used to highlight molecules with

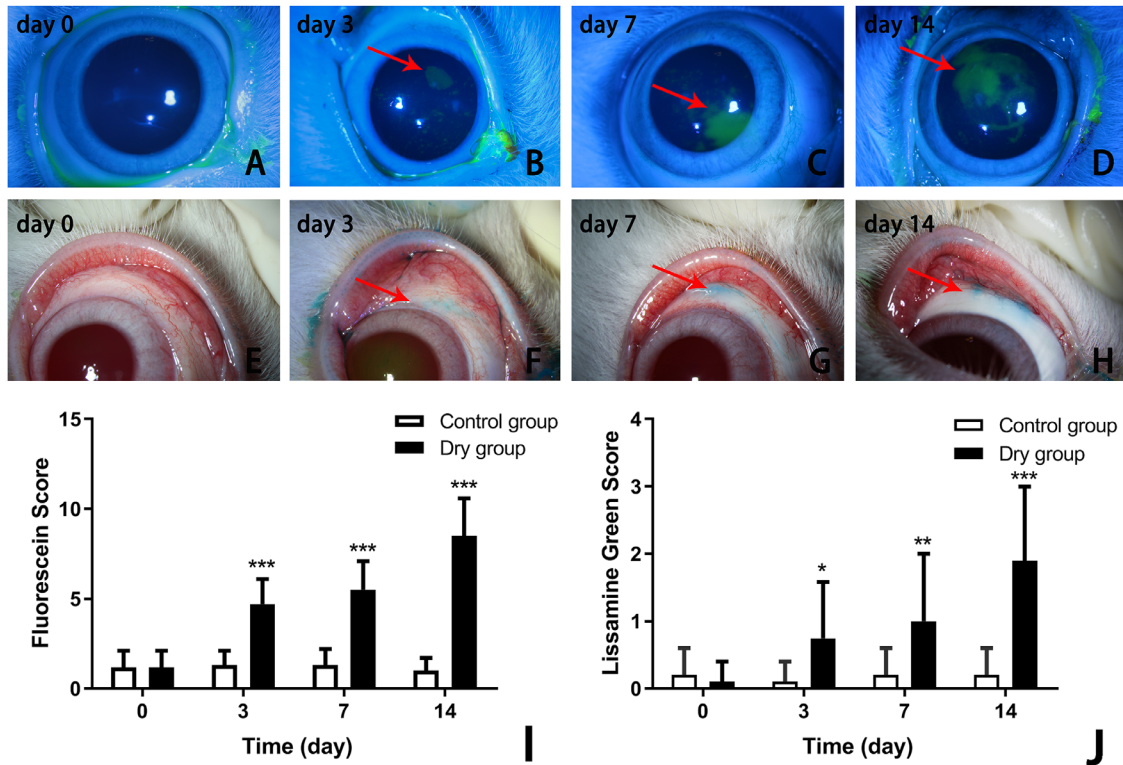


Figure 3. Comparison of corneal fluorescein staining and conjunctival lissamine green staining of the control and dry groups at different times selected randomly from the same batch of parallel experiments. There was no fluorescein staining or lissamine green staining on the ocular surface on day 0 in the dry group and control group at all time points (A, E). From day 3, the corneal fluorescein staining and conjunctival lissamine green staining presented in the dry group (B–D; F–H). The corneal fluorescein staining increased over time in the dry group (I; *** $P < 0.001$, $n = 12$ [24 eyes] each group). There was a statistical difference in the conjunctival lissamine green staining between the dry and control groups on days 3, 7, and 14 (J; * $P < 0.05$, ** $P < 0.01$, *** $P < 0.001$, respectively, $n = 12$ [24 eyes] per group). Data are shown as mean \pm SD.

a high percentage of mucin. On day 14, the average number of goblet cells in the superior bulbar conjunctiva was 15 ± 4 and 10 ± 2 in the control group and dry group, respectively (Figs. 5A, 5B). The number of conjunctival goblet cells in the dry group was significantly lower than that in the control group ($t = 4.162$, $P < 0.01$, $n = 4$ [8 eyes] per group, Fig. 5C).

The MUC5AC protein is an important part of the tears secreted by goblet cells. The expression of MUC5AC in the conjunctival epithelium was detected via immunofluorescence staining. The results showed that, in the control experiment, no cells were marked with green fluorescence in the conjunctival epithelium in the control group (Fig. 6A) and the dry group (Fig. 6B). There were no positive stained cells in the cornea (Fig. 6C). MUC5AC-stained positive cells were more greatly decreased in the dry group than in the control group on day 14 ($0.35\% \pm 0.16\%$ vs. $0.08\% \pm 0.03\%$; $t = 3.707$, $P < 0.01$, $n = 3$ [6 eyes] per group, Figs. 6D–F).

Evaluation of Cellular Apoptosis in Cornea, Conjunctiva, and Lacrimal Gland

Caspase-3 is a type of protein activated by apoptosis. The expression of the caspase-3 protein in the ocular surface tissues and lacrimal glands was detected via immunohistochemistry. In the control experiment, no cells in the control group and the dry group were positive in the corneal epithelium (Figs. 7A, 7B), conjunctival epithelium (Figs. 7F, 7G), and lacrimal gland (Figs. 7K, 7I). On day 14, the percentages of IOD were significantly higher in the dry group than in the control group in the corneal epithelium ($0.21\% \pm 0.03\%$ vs. $0.17\% \pm 0.02\%$, respectively; $t = -4.401$, $P < 0.01$, $n = 3$ [6 eyes] per group, Figs. 7C–E) and conjunctival epithelium ($0.84\% \pm 0.15\%$ vs. $0.55\% \pm 0.16\%$; $t = -2.882$, $P < 0.05$, $n = 3$ [6 eyes] per group, Figs. 7H–J). However, the IOD percentage of the caspase-3 protein did not show any significant difference between these two groups in the lacrimal gland ($11\% \pm 3\%$ in the

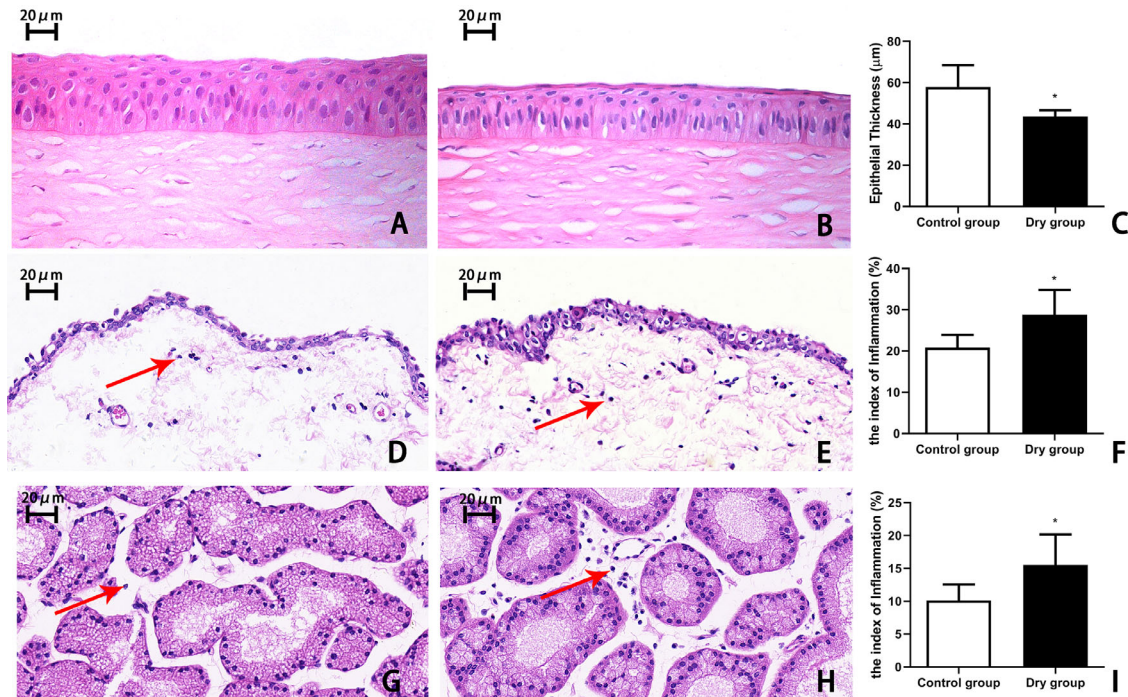


Figure 4. Representative images and histological analysis of the cornea, conjunctiva, and lacrimal gland on day 14. (A) The corneal epithelium in the control group was well-stratified with five to six cells layers. (B) In contrast, the corneal epithelium in the dry group had three to four layers, and (C) was statistically thinner than that of the control (* $P < 0.05$, $n = 4$ [8 eyes] each group). A greater number of inflammatory cells (red arrows) was observed in the conjunctiva of the dry group (E) than in the control group (D). (F) There was a more significant increase in the index of inflammation in the conjunctiva of the dry group than the control group (* $P < 0.05$, $n = 4$ [8 eyes] per group) (G–I). The lacrimal gland of the dry group had more and more infiltrated inflammatory cells over time compared with the control group (* $P < 0.05$, $n = 4$ [8 eyes] each group). Data are shown as mean \pm SD. Magnification, $\times 400$.



Figure 5. The number of goblet cells in rabbit conjunctiva on day 14. The goblet cells were stained pink (arrows) by PAS in the conjunctival epithelium of the normal rabbits (A). The epithelium had fewer goblet cells in the rabbit conjunctiva after 14 days of treatment in the CDS (B, C; ** $P < 0.01$, $n = 4$ [8 eyes] per group).

control group vs. $10\% \pm 2\%$ in the control group; $t = 0.6659$, $P > 0.05$, $n = 3$ [6 eyes] per group, Figs. 7M–O).

Expression Levels of IL-1 β , TNF- α , and MMP-9 mRNA

The expression levels of IL-1 β , TNF- α , and MMP-9 mRNA changed in the rabbit ocular surface and lacrimal gland on day 14 after placement of the dry

environment. There were no statistically significant differences in the control group throughout the study period. In the cornea, the levels of IL-1 β , TNF- α , and MMP-9 were more significantly increased in the dry group than in the control group (IL-1 β : 1.00 ± 0.21 vs. 2.31 ± 1.48 , $t = -2.741$, $P < 0.01$; TNF- α : 0.96 ± 0.27 vs. 3.08 ± 3.52 , $t = -1.202$, $P < 0.05$; MMP-9: 1.00 ± 0.27 vs. 2.20 ± 0.90 , $t = -2.537$, $P < 0.05$, $n = 5$ [10 eyes] per group, respectively; Fig. 8A). In the conjunctiva, the levels of IL-1 β and TNF- α in the dry group were

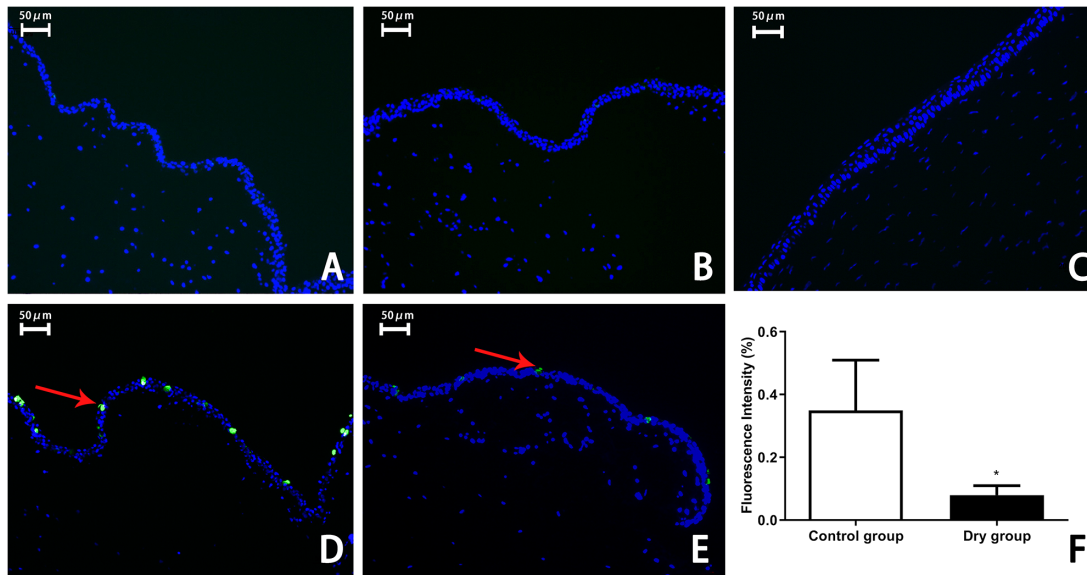


Figure 6. Representative images with immunofluorescence and histological analysis of MUC5AC in the conjunctival epithelium on day 14. Control experiment showed no green fluorescence in the conjunctival epithelium in the control group (A) and the dry group (B). No positive stained cells were observed in the cornea (C), which served as a negative control. The expression of the MUC5AC protein was marked with green fluorescence (arrows) in the conjunctival epithelial cytoplasm of the normal rabbits (D). In the dry group, fewer cells with green fluorescence were noted in the conjunctival epithelium on day 14 (E, F; $^{**}P < 0.01$, $n = 3$ [6 eyes] per group). Data are shown as mean \pm SD (error bars). Magnification, $\times 200$.

significantly higher than in the control group (IL-1 β : 1.00 ± 0.83 vs. 2.60 ± 1.26 , $t = -2.40$, $P < 0.05$; TNF- α : 0.31 ± 0.96 vs. 4.60 ± 5.07 , $t = -1.425$, $P < 0.05$; MMP-9: 1.02 ± 0.31 vs. 1.86 ± 1.29 , $t = -1.425$, $P > 0.05$; $n = 5$ [10 eyes] per group, respectively; Fig. 8B). In the lacrimal gland, there was no statistically significant difference in the levels of IL-1 β , MMP-9, and TNF- α between groups (1.41 ± 1.11 vs. 2.23 ± 1.76 , $t = 0.7949$, $P > 0.05$; 2.31 ± 3.15 vs. 3.72 ± 4.98 , $t = -2.621$, $P < 0.05$; 1.21 ± 0.76 vs. 6.35 ± 3.84 , $t = 0.481$, $P > 0.05$; $n = 5$ [10 eyes] per group, respectively; Fig. 8C).

Discussion

Environmental factors, such as humidity, AF, and T, can change the dynamic characteristics of tear film and thus affect the ocular surface.¹⁵ To study the influence of the dry environment on the ocular surface, environment-induced animal dry eye was first induced in mice in a controlled-environmental chamber by Barabino et al.⁷ However, there has not been a system reported for the successful creation of rabbit dry eye in consideration of the frequent excrement of urine and the size limit of the previous system. Herein, we modified the dry environment production system, which was suitable for developing a dry eye model in

rabbits. In this new CDS, the air in the cage could be constantly maintained at a designated and adjustable humidity for the induction of dry eye in rabbits—and even other large animals.

The CDS was designed to provide stable airflow into six separate cages at the same time. The air humidity could be adjusted to a designated set lower than the room set. During the experiment, it was best to set the AF at 3 to 4 m/s to constantly provide a low-humidity environment of $22\% \pm 4\%$ in the cages. In this system, the AF did not directly blow into the animals' eyes, which was to mimic human patients in their daily life or work. To manage the humidity in the cages more effectively, additional elements such as a compressed air fine filter, several dry columns, and an upper iron mesh layer with desiccants for further dehumidification were incorporated into the system. A concave element was attached to the bottom of each cage, with a hole in the center for quick discharge and the self-cleaning of rabbit urine over time. The parameters of humidity, T, and AF speed in the cages were wirelessly monitored and real-time recorded. Furthermore, to avoid the protective effect of rabbit nictitating membrane on the establishment of dry eye, it was cut off before the experiment. The nictitating membrane can cover two-thirds of the cornea acting as a mechanical barrier, such as a contact lens.^{16–18}

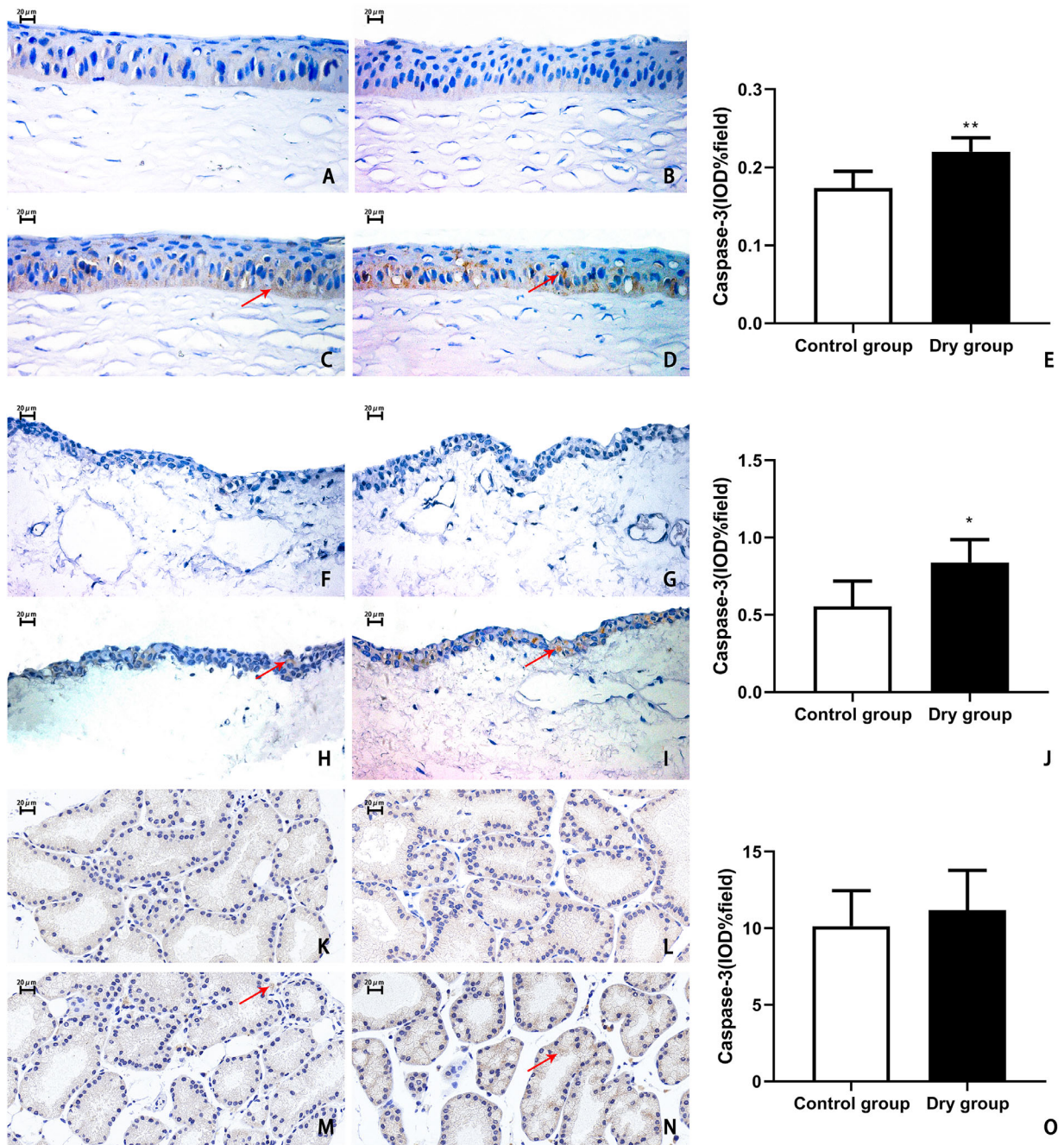


Figure 7. Representative images and histological analysis of caspase-3 in the corneal epithelium, conjunctival epithelium, and lacrimal gland on day 14. Control experiment showed no positive stained cells in the corneal epithelium (A, B), conjunctival epithelium (F, G), and lacrimal gland (K, L) in the control group and the dry group. On day 14, in the control group, there were little apoptotic cells in the corneal epithelium (C), conjunctival epithelium (H), and lacrimal gland (M). In the dry group, the caspase-3-positive cells in the cornea (D, E) and conjunctiva (I, J) were more significantly increased than in the control group (cornea, $**P < 0.01$, $n = 3$ [6 eyes] per group; conjunctiva, $*P < 0.05$, $n = 3$ [6 eyes] per group). There were no statistically significant differences in the lacrimal glands (N, O) between these two groups ($P > 0.05$, $n = 3$ [6 eyes] each group). Data are shown as mean \pm SD (error bars). Magnification, $\times 400$.

The most common indicators for diagnosing human dry eye are the decrease in tear production and damage to the ocular surface epithelium, which are also applicable in animal dry eye. In our study, the rabbits housed

in the CDS for 14 days suffered from a significant decrease in tear secretion accompanied by a significant defect in the corneal and conjunctival epithelium from day 3. These changes were consistent with the results

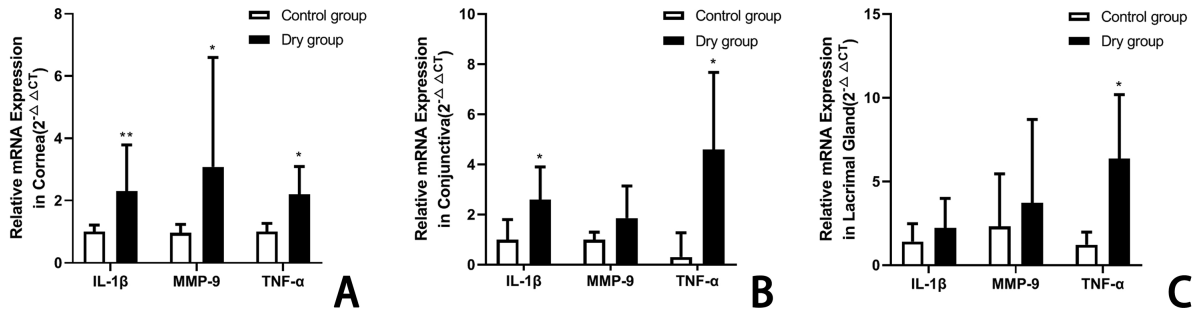


Figure 8. The mRNA expression levels of IL-1 β , TNF- α , and MMP-9 in rabbit cornea (A), conjunctiva (B), and lacrimal gland (C) on day 14. In the cornea, the levels of IL-1 β , TNF- α , and MMP-9 were more significantly increased in the dry group than in the control group (** $P < 0.01$, * $P < 0.05$, * $P < 0.05$; $n = 5$ [10 eyes] per group). In the conjunctiva, the levels of IL-1 β and TNF- α in the dry group were remarkably higher than in the control group (* $P < 0.05$, * $P < 0.05$; $n = 5$ [10 eyes] per group). In the lacrimal gland, the TNF- α levels in the dry group were statistically greater than in the control group (* $P < 0.05$, $n = 5$ [10 eyes] per group). Data are shown as mean \pm SD (error bars). All data represent the relative fold change in the mRNA expression levels.

of murine models in the CEC or ICES, and similar to the dry eye symptoms of human patients exposed to a dry environment.^{7,8,11} The corneal epithelium of the rabbits gradually thinned, and the number of conjunctival goblet cells significantly decreased. These pathological changes were similar to those found in rabbit dry eye induced by the topical application of benzalkonium chloride,¹⁹ which was similar to the clinical manifestation of human dry eye.^{4-6,20}

Inflammation was considered one of the core pathogenesis in the development of dry eye.²¹ Proof of inflammation has been documented in human patients with dry eye. The infiltration of inflammatory cells was demonstrated in the conjunctiva and lacrimal glands.²²⁻²⁷ In this study, many inflammatory cells were also infiltrated in the conjunctiva and lacrimal gland after housing in a low-humidity environment. Meanwhile, the levels of inflammatory cytokines, such as IL-1 β , TNF- α , and MMP-9 mRNA, in the ocular surface tissues were also significantly increased to different degrees, which was consistent with the changes seen in patients with dry eye.²²⁻²⁷ Inflammation is a critical cause and effect of ocular surface dryness and injury, which may lead to epithelial apoptosis.²⁸⁻³⁰ However, in the lacrimal glands of rabbit environment dry eye, there was no statistically significant difference in the mRNA levels of IL-1 β , MMP-9, and TNF- α expression, even though there was infiltration of some of the inflammatory cells in this study. This result was also observed in the environment of mice dry eye reported by Xiao et al.³¹ These results suggested that dry environment-induced dry eye may mainly induced local effects on the ocular surface while failing to elicit lacrimal gland inflammation.

Epithelial apoptosis has been suggested as contributing to the pathogenesis of dry eye.³²⁻³⁴ Our results showed that a dry environment induces more apoptotic proteins of caspase-3 in rabbit cornea and conjunctiva but not in the lacrimal gland. These results indicate that a continuous dry environment would lead to the infiltration of inflammatory cells and damage in the ocular surface, causing the apoptosis of the ocular epithelial cells.³⁵

The tear film contains a variety of mucins adjacent to the glycocalyx of the apical cells of the ocular epithelium. According to their physiologic functions, they can be classified as gel-forming mucins, soluble mucins, and membrane-spanning mucins.³⁶ MUC5AC in tears is one of the major secreted gel-forming mucins and is a product of conjunctival goblet cells.³⁷ It was spread by eyelid movement during blinking to maintain the wettability and lubrication of ocular surface. A number of studies suggested that MUC5AC may be a potential indicator for the diagnosis of dry eye in human and animal dry eye.³⁸ After being housed in a dry environment, the rabbits showed lesser goblet cell density than in the normal environment. The tear film was unstable and instigated dry eye because the number of MUC5AC protein continuously decreased, which would induce a vicious unstable tear film-inflammatory damage cycle.³⁹

Based on the experimental data, the dry eye model in this study is an evaporative subtype and consistent with human environmental dry eye. Using this CDS, it took 2 weeks to create rabbit dry eye. To date, several animal models have been established for investigation of evaporative dry eye. Barabino et al.⁷ induced a mouse dry eye model through a CEC for the first time. Then Chen et al.⁸ designed an intelligent system

to improve the maintenance of humidity, air velocity, and temperature. These two systems were developed for mice, and it usually takes 4 weeks to create dry eye. Another evaporative dry eye model was developed by Gilbard et al.⁴⁰ through closure of rabbit meibomian gland orifices by cautery. In this model, the meibomian gland function was irreversibly damaged. Moreover, Fujihara et al.⁴¹ introduced an acute rabbit dry eye model by mechanical prevention of blinking.

Conclusions

This study developed an aqueous-deficient dry eye model in rabbits through the CDS that was able to create and maintain a dry environment. The pathological changes in rabbit environmental dry eye induced in the CDS were highly similar to that in human evaporative dry eyes. This model is suitable for investigating the effect of a dry environment on ocular surface homeostasis, the pathophysiology of environment-induced dry eye, and its potential treatment.

Acknowledgments

The authors thank Jian Dong Luo (South China University of Technology, Guangzhou, China) and Jian Cheng Zhan (ShenZhen DJI Technology Co., Ltd, Shenzhen, China) for their valuable suggestions regarding designing the CDS.

Partly supported by the National Science Funding of China (Grant number: 31671210) and the Fundamental Research Funds of the State Key Laboratory of Ophthalmology (Grant number: 30306020240020149) in China. The sponsors or funding organizations had no roles in the design or conduct of this research.

Disclosure: **X.-M. Chen**, None; **J.-B. Kuang**, None; **H.-Y. Yu**, None; **Z.-N. Wu**, None; **S.-Y. Wang**, None; **S.-Y. Zhou**, None

* X-MC and J-BK contributed equally to this work.

References

1. Bron AJ, dePaiva CS, Chauhan SK, et al. TFOS DEWS II pathophysiology report. *Ocul Surf*. 2017;15:438–510.
2. Li J, Tan G, Ding X, et al. A mouse dry eye model induced by topical administration of the air pollutant particulate matter 10. *Biomed Pharmacother*. 2017;96:524–534.
3. Johnson ME, Murphy PJ. Changes in the tear film and ocular surface from dry eye syndrome. *Prog Retin Eye Res*. 2004;23:449–474.
4. Backman H, Haghighat F. Indoor-air quality and ocular discomfort. *J Am Optom Assoc*. 1999;70:309–316.
5. Backman H, Haghighat F. Air quality and ocular discomfort aboard commercial aircraft. *Optometry*. 2000;71:653–656.
6. Sommer HJ, Johnen J, Schöngen P, Stolze HH. Adaptation of the tear film to work in air-conditioned rooms. *Ger J Ophthalmol*. 1994;3:406–408.
7. Barabino S, Shen L, Chen L, et al. The controlled-environment chamber: a new mouse model of dry eye. *Invest Ophthalmol Vis Sci*. 2005;46:2766–2771.
8. Chen W, Zhang X, Zhang J, et al. A murine model of dry eye induced by an intelligently controlled environmental system. *Invest Ophthalmol Vis Sci*. 2008;49:1386–1391.
9. Short BG. Safety evaluation of ocular drug delivery formulations: techniques and practical considerations. *Toxicol Pathol*. 2008;36:49–62.
10. Zernii EY, Baksheeva VE, Iomdina EN, et al. Rabbit models of ocular diseases: new relevance for classical approaches. *CNS Neurol Disord Drug Targets*. 2016;15:1–25.
11. Lemp MA. Report of the National Eye Institute/industry workshop on clinical trials in dry eyes. *CLAO J*. 1995;21:221–232.
12. Bron AJ, Evans VE, Smith JA. Grading of corneal and conjunctival staining in the context of other dry eye tests. *Cornea*. 2003;22:640–650.
13. Bhattacharya D, Shen L, Chen L, et al. Tear production after bilateral main lacrimal gland resection in rabbits. *Invest Ophthalmol Vis Sci*. 2015;56:7774–7783.
14. Li G, Lu P, Song H, Zheng Q, Nan K. Expression of mucins MUC5AC and MUC19 on the ocular surface in dry eye syndrome model of ovariectomized female rabbits. *Adv Clin Exp Med*. 2019;28:165–169.
15. Rolando M, Refojo MF. Tear evaporimeter for measuring water evaporation rate from the tear film under controlled conditions in humans. *Exp Eye Res*. 1983;36:25–33.
16. Davis FA. The anatomy and histology of the eye and orbit of the rabbit. *Trans Am Ophthalmol Soc*. 1929;27:400.2–441.
17. Umeda Y, Nakamura S, Fujiki K, Toshida H, Saito A, Murakami A. Distribution of goblet cells and MUC5AC mRNA in the canine nictitating membrane. *Exp Eye Res*. 2010;91(5):721–726.

18. Hendrix DVH. Canine conjunctiva and nictitating membrane. In: Gelatt KM, ed. *Vet Ophthalmol. Canine Conjunctiva and Nictitating Membrane*. 24th ed. Ames, IA: Blackwell; 2007:675.
19. Xiong C, Chen D, Liu J, et al. A rabbit dry eye model induced by topical medication of a preservative benzalkonium chloride. *Invest Ophthalmol Vis Sci*. 2008;49(5):1850–1856.
20. Kunert KS, Tisdale AS, Gipson IK. Goblet cell numbers and epithelial proliferation in the conjunctiva of patients with dry eye syndrome treated with cyclosporine. *Arch Ophthalmol*. 2002;120:330–337.
21. Nai-Wen F, Dohlman TH, Foulsham W, et al. The role of Th17 immunity in chronic ocular surface disorders. *Ocul Surf*. 2021;19:157–168.
22. Peters A. Epidemiology: air pollution and mortality from diabetes mellitus. *Nat Rev Endocrinol*. 2012;8(12):706–707.
23. Cadelis G, Tourres R, Molinie J. Short-term effects of the particulate pollutants contained in Saharan dust on the visits of children to the emergency department due to asthmatic conditions in Guadeloupe (French Archipelago of the Caribbean). *PLoS One*. 2014;9(3):e91136.
24. Rogula-Kozłowska W. Size-segregated urban particulate matter: mass closure, chemical composition, and primary and secondary matter content. *Air Qual Atmos Health*. 2016;9:533–550.
25. Pei Y, Jiang R, Zou Y, et al. Effects of fine particulate matter (PM_{2.5}) on systemic oxidative stress and cardiac function in apoE(–/–) mice. *Int J Environ Res Public Health*. 2016;13(5):484.
26. Samoli E, Peng R, Ramsay T, et al. Acute effects of ambient particulate matter on mortality in Europe and North America: results from the APHENA study. *Environ Health Perspect*. 2018;116(11):1480–1486.
27. Galor A, Kumar N, Feuer W, Lee DJ. Environmental factors affect the risk of dry eye syndrome in a United States veteran population. *Ophthalmology*. 2014;121(4):972–973.
28. Ru Y, Huang Y, Liu H, et al. Alpha-melanocyte-stimulating hormone ameliorates ocular surface dysfunctions and lesions in a scopolamine-induced dry eye model via PKA-CREB and MEK-Erk pathways. *Sci Rep*. 2015;5:18619.
29. Pflugfelder SC, Corrales RM, de Paiva CS. T helper cytokines in dry eye disease. *Exp Eye Res*. 2013;117:118–125.
30. McNamara Na, Gallup M, Porco TC. Establishing PAX6 as a biomarker to detect early loss of ocular phenotype in human patients with Sjogren's syndrome. *Invest Ophthalmol Visual Sci*. 2014;55(11):7079–7084.
31. Xiao B, Wang Y, Reinach PS, et al. Dynamic ocular surface and lacrimal gland changes induced in experimental murine dry eye. *PLoS One*. 2015;10(1):1–8.
32. Seo Y, Ji YW, Lee SM, et al. Activation of HIF-1alpha (hypoxia inducible factor-1alpha) prevents dry eye-induced acinar cell death in the lacrimal gland. *Cell Death Dis*. 2014;5:e1309.
33. Lai CT, Yao WC, Lin CY, et al. Changes of ocular surface and the inflammatory response in a rabbit model of short-term exposure keratopathy. *PLoS One*. 2015;10(9):e0137186.
34. Lee HS, Cui L, Li Y, et al. Influence of light emitting diode-derived blue light overexposure on mouse ocular surface. *PLoS One*. 2016;11(8):e0161041.
35. Yamaguchi T. Inflammatory response in dry eye. *Invest Ophthalmol Vis Sci*. 2018;59:DES192–DES199.
36. Moniaux N, Escande F, Porchet N, Aubert JP, Batra SK. Structural organization and classification of the human mucin genes. *Front Biosci*. 2001;6:D1192–D1206.
37. McKenzie RW, Jumblatt JE, Jumblatt MM. Quantification of MUC2 and MUC5AC transcripts in human conjunctiva. *Invest Ophthalmol Vis Sci*. 2000;41(3):703–708.
38. Hori Y. Secreted mucins on the ocular surface. *Invest Ophthalmol Vis Sci*. 2018;59:DES151–DES156.
39. Stephens DN, McNamara NA. Altered mucin and glycoprotein expression in dry eye disease. *Optom Vis Sci*. 2015;92:931–938.
40. Gilbard JP, Rossi SR, Heyda KG. Tear film and ocular surface changes after closure of the meibomian gland orifices in the rabbit. *Ophthalmology*. 1989;96(8):1180–1186.
41. Fujihara T, Nagano T, Nakamura M, Shirasawa E. Establishment of a rabbit short-term dry eye model. *J Ocul Pharmacol Ther*. 1995;11(4):503–508.